Interaction of Si, Ge, and Be solutes with vacancies and interstitials in Ni

Raju P. Gupta

Centre d'Etudes Nucléaires de Saclay, Section de Recherches de Métallurgie Physique, Boîte Postale n°2, 91190 Gif sur Yvette, France

(Received 14 August 1979; revised manuscript received 9 June 1980)

The solute-vacancy and the solute-interstitial binding energies for Si, Ge, and Be solutes in Ni matrix have been calculated, using the results of an augmented-plane-wave calculation of the electronic structure of the solute and the solvent atoms. The electronic wave function of the solute is expressed in terms of the wave functions of the unperturbed host lattice. This allows the partial densities of states (DOS) of different angular momentum type at the solute site to be written in terms of those at the solvent atom site and their energy-dependent phase shifts. It is found that the *d* electron DOS which is large and dominant at the Ni site is rather small at the solute site for all the solutes studied here. At the Si and Ge sites the *p* DOS is dominant while at the Be site both *s* and *p* components are important. The excess charge density displaced by the solute and the potential associated with it show the oscillatory behavior. The 3*s* and 4*s* electrons of Si and Ge, respectively, form bound states below the bottom of the Ni conduction band. These states influence in a profound manner the interaction of these solutes with both vacancies and interstitials. No bound state is formed in the case of Be, where the scattering states in the conduction band are the sole contributors to the interaction energy. We have found that Ge, even though oversized, has a positive binding energy of 0.28 eV with the interstitial in the mixed dumbbell configuration. The undersized Si and Be form mixed dumbbells with binding energies of 0.90 and 0.58 eV, respectively. Contrary to usual expectations the vacancy-solute binding is calculated to be rather strong, 0.73 and 0.55 eV, respectively, for Si and Ge in the nearest-neighbor vacancy-solute configuration. The corresponding interaction with Be is found to be repulsive with a binding energy of -0.32 eV.

I. INTRODUCTION

The interaction of solute atoms with vacancies and interstitials is of paramount importance in the production, migration, and agglomeration of radiation-induced defects and in the growth of voids and dislocation loops. The vacancy-solute interaction also plays an important role in the thermal atomic diffusion, and a knowledge of its role could aid in the calculation of various atomic jump frequencies. As a result, investigations which can shed light on the nature of these interactions are of substantial interest, not only scientifically but also from a technological standpoint. Experimentally, the binding energies of solutes with interstitials or vacancies are available only in very few cases, essentially for some solutes in Al and Cu,[1-7] because, in part, of the difficulty in performing such experiments and sometimes because of the ambiguity and difficulty in the interpretation of the experimental data.[8,9] Theoretical effort in this area has also been rather limited.[2,5-7,10] As a result, systematic studies of the effect of minor solute additions on the performance capability of pure metals and alloys under irradiation do not exist. In this paper an approach is presented which permits the evaluation of the solute-interstitial and the solute-vacancy binding energies from a knowledge of the electronic band structure of the host matrix.

We will recall briefly the most salient features of the theoretical models which are available at the present time in order to obtain estimates of the interaction energy of a solute with either vacancies or interstitials. The experimental data on solute segregation, precipitation, void swelling, etc., in irradiated metals containing small amounts of a solute are usually interpreted in terms of the size of the solute in the matrix.[2,11,12] The dominating nature of the effect of the solute size arises from the strain-field considerations, and one assumes that it is energetically favorable for the undersized solutes to form mixed ⟨100⟩ dumbbells. While for oversized solutes the formation of mixed dumbbells is ruled out, these solutes are considered to have a positive binding energy with a vacancy. Dederichs *et al.*[2] have exploited the size effect of a solute to determine quantitatively its interaction with interstitials in the mixed ⟨100⟩ dumbbell and other configurations. The principal ingredient of their model is the Cu interatomic potential of the classical Morse type which represents the host-host potential. The interaction of a solute atom with a host atom is simulated by shifting the Cu interatomic potential by an amount r_0 which is proportional to the linear size factor (lsf) of the solute in the host. A tabulation of the lsf for a number of solutes in different matrices is given by King.[13] The binding energy of the solute in this model is found to be essentially proportional to the lsf of the solute. Not surprisingly, the model predicts the formation of the mixed ⟨100⟩ dumbbells for the undersized solutes. The quantitative estimates of the binding energies obtained from

this model will have to be taken with caution for the following two obvious reasons: First, the Cu interatomic potential can hardly be expected to represent an appropriate choice for another face-centered-cubic (fcc) metal of interest. This difficulty can be remedied by choosing an interatomic potential which is appropriate to the host metal. However, in this connection we note here that Johnson[14] has pointed out that his attempts to construct a suitable interatomic potential for gold have not met with success. Second, due to the nonavailability of the solute-host interatomic potentials, it is perhaps convenient to represent the solute-host potential by a mere shift of the host-host interatomic potential; this is, nevertheless, a rather drastic approximation and hard to justify. The calculations of Johnson *et al.*[15] for the Fe-C and Fe-Fe interatomic potentials indicate that the Fe-C potential cannot be obtained by a simple shift of the Fe-Fe interatomic potential.

Indeed, the relationship between the solute size and its role in the formation of mixed dumbbells should be more fully investigated. Experimental evidence suggesting such a relationship is rather indirect and based only on a few solutes in Cu and Al. Direct experimental observation of the formation of the mixed ⟨100⟩ dumbbells for undersized solutes by Swanson *et al.*[16] has recently been questioned by Rehn *et al*[18]; presumably because the solute concentration used in the channeling studies of Swanson *et al.* was large, and because there are inherent difficulties in the channeling technique in distinguishing between contributions from different defect configurations simultaneously present in the sample. Setser *et al.*[17] have performed ultrasonic attenuation experiments on Al-100-ppm Fe and Al-800-ppm Mn systems under electron irradiation and have found that even though Fe and Mn have similar size differences with Al, the results for the two alloy systems are very different, contrary to expectations from existing theory. Marwick *et al.*[18] have noted that their results on the segregation of Al, Cr, Mn, and Ti in Ni under Ni^+ irradiation could be better described if a small binding (~0.1 eV) between these solutes and the interstitials leading to the formation of a transient dumbbell could be assumed, even though they are oversized in Ni with linear size factors of 4.67, 3.33, 7.20, and 8.97%, respectively. We note also a frequently overlooked case: Ag in Al. Despite the fact that Ag is slightly oversized in Al (lsf of 0.03%) it has been concluded that Ag forms a strong trap in Al which is stable up to stage III.[16] These departures from the empirical relationship between the solute size and its interaction with interstitials are in fact not unexpected. Even though the size of a solute and its interactions with defects in a matrix are both determined by its electronic structure, each represents a macroscopic quantity involving different microscopic averages and a direct relationship between the two cannot be established. Even though W and In have the same lsf (~11%) in Ni, Cr, and Pb in Al (~−23 to −25%), Cu and V in Al (~−15 to −16%), Ge and Pd in Cu (~8.6%), etc., it will be indeed very hard to understand that these solutes will interact in an identical manner with an interstitial atom in the lattice, despite the fact that they are electronically very different from each other.

The work on the problem of solute-vacancy interactions has similarly been rather limited, especially from a theoretical point of view.[3-7,9,10] Experimental values of binding energies are available mostly for solutes in Al and for some solutes in Cu. There is a wide discrepancy between values determined by different techniques, but the general conclusion is that the solute-vacancy binding energies are small for most solutes in Al, except the transition-metal solutes. As reliable values for other systems are lacking it is now generally believed, on the basis of results in Al, that the solute-vacancy binding energy is generally rather small. Indeed, this view has been taken over in the interpretation of the experimental data on solute segregation and precipitation under irradiation.[19] Theoretically, the pseudopotential method has been used recently to calculate the solute-vacancy binding energies for simple-metal solutes in Al.[7,20] However, the results obtained from these calculations are very sensitive to the choice of the pseudopotential. This has been demonstrated recently[21] for the case of Al(Zn), as an example, where the use of two different pseudopotentials for Al resulted not only in a different strength of the Zn-vacancy binding energy but also in a change of sign. The values also depend sensitively on the choice of the corrections for exchange and correlations employed in the linear dielectric screening function.[22] Apart from these drawbacks the method has a rather limited applicability since it can be used to study only the simple-metal solutes in simple-metal hosts.

The most promising approach appears to be that of Blandin, Déplanté, and Friedel,[23,24] who have employed the scattering theory to calculate the solute-vacancy binding energies in Cu. Their method is not restricted to simple-metal solutes, and calculations have been performed for both simple- and transition-metal solutes in Cu and Al.[5] The host matrix for Cu and Al studied so far has been represented by a free-electron gas; the band-structure effects are thus not included.

Within the asymptotic approximation[25] for the electron wave functions, and assuming that the phase shifts vary slowly as a function of energy, one finds that the excess electron density displaced by the solute and the excess potential created have exactly the same form, except for a constant multiplicative factor which is both simple and analytic and which depends essentially on the phase shift η_l^s of the solute evaluated at the Fermi energy of the host. The vacancy is represented by a point charge, and one finds that the solute-vacancy interaction energy is not limited to nearest neighbors but has a rather long-range oscillatory character.

In spite of these approximations the results obtained from this model are rather encouraging. The calculation of the migration and the activation energies using Le Claire's[26] split-vacancy model, where one assumes a vacancy in the saddle-point configuration to be represented by two half-vacancies each represented by a point charge one-half that of the original vacancy, shows in general a trend in agreement with experiment. Let us note here that because of the very small separation between a half-vacancy and the solute ($\frac{11}{16}$ of the nearest-neighbor separation) the asymptotic approximation is worse here than in the calculation of the solute-vacancy binding energies.

In view of the apparent success of this model in predicting experimental trends it is clearly preferable to retain the basic structure of this model and to ameliorate it by avoiding some of the more questionable approximations. This is indeed the purpose of the present paper. One expects the inclusion of the proper nonasymptotic form of the wave functions and the variation of the phase shifts throughout the Fermi sea to result in more accurate results. This in turn requires a knowledge of the band structure and wave functions of the host matrix. These modifications of the theory allow it to be extended to include the case of transition-metal solvents. We show that the charge density displaced by the solute depends on the detailed structure of the densities of states (DOS) of different angular momentum types at the solvent and the solute atom sites. The detailed electronic structures of the solvent and the solutes and the effects due to s-d hybridization are also included. The unperturbed host is treated here in the muffin-tin approximation. The introduction of the solute is assumed to perturb the crystalline potential only within the muffin-tin sphere centered on the solute site.

In the work reported here the solute-vacancy binding energies of Si, Ge, and Be solutes in Ni matrix in its paramagnetic phase are calculated. We have also used this theory to calculate the solute-interstitial binding energies in the mixed-dumbbell configuration. Section II is devoted to the description of the method. Expressions for the excess electron density and the electronic potential are derived which are then used in the calculations of the interaction energy of the solute with vacancies and interstitials. Electronic structure of the Si, Ge, and Be solutes in Ni are discussed in Sec. III and the results on interaction energies are given in Sec. IV. Concluding remarks are given in Sec. V.

II. FORMULATION

In order to calculate the electron density displaced by the solute we make use of the muffin-tin approximation.[27-29] The wave function inside the muffin-tin sphere at the solvent atom site at origin in the perfect crystal may be written as

$$\psi_k(\vec{r}) = \sum_{l\,m} a_{l\,m}(k) R_l(E, r) y_{l\,m}(\hat{r}) , \tag{1}$$

where $R_l(E, r)$ is the solution of the radial Schrödinger equation with the host muffin-tin potential at energy E, $a_{l\,m}$ are the expansion coefficients, $\hat{r} = \vec{r}/r$, and the index k includes both the wave vector $\vec{k}$ and the band index n. R_l is normalized so that $R_l(E, R) = 1$, where R is the muffin-tin radius. Outside R, ψ_k is expressed in terms of spherical waves so that it matches the solution from inside smoothly at R. This gives (for $r > R$)

$$\psi_k(r) = \sum_{l\,m} a_{l\,m}(k) \frac{1}{N_l(K, R)} [j_l(Kr)\cos\delta_l(E) - n_l(Kr)\sin\delta_l(E)] y_{l\,m}(\hat{r}) , \tag{2}$$

where $K = \sqrt{E}$, $\delta_l(E)$ is the phase shift of host muffin-tin potential at energy E, and

$$N_l(K, R) = j_l(K, R)\cos\delta_l(E) - n_l(K, R)\sin\delta_l(E) , \tag{3}$$

with j_l and n_l being the spherical Bessel and Neumann functions, respectively.

The wave functions ψ_k^s at the solute site are expressed as a sum of two waves,[30-33] the function ψ_k and an outgoing spherical wave ψ^s,

$$\psi_k^s(\vec{r}) = \psi_k(\vec{r}) + \psi^s(\vec{r}) , \tag{4}$$

and following Morgan,[30] ψ^s is expressed in terms of Hankel functions h_l ($h_l = j_l + in_l$):

$$\psi^s(\vec{r}) = \sum_{l\,m} b_{l\,m} h_l(Kr) y_{l\,m}(\hat{r}) . \tag{5}$$

Inside the muffin-tin sphere of the solute, which we place at the origin, the wave function may alternatively be expanded in spherical waves

$$\psi_k^s(\vec{r}) = \sum_{l\,m} C_{l\,m}(k) R_l^s(E, r) y_{l\,m}(\hat{r}), \tag{6}$$

where R_l^s is the radial wave function at the solute site determined from the muffin-tin potential of the solute. Outside the muffin-tin sphere, $\psi_k^s(\vec{r})$ may be expanded in a manner similar to Eq. (2),

$$\psi_k^s(\vec{r}) = \sum_{l\,m} C_{l\,m}(k) \frac{1}{N_l^s(K, R)} [j_l(Kr)\cos\delta_l^s(E) - n_l(Kr)\sin\delta_l^s(E)] y_{l\,m}(\hat{r}), \tag{7}$$

where δ_l^s is the phase shift of the solute potential and N_l^s is obtained from Eq. (3) by replacing δ_l by δ_l^s.

The coefficients $b_{l\,m}$ and $C_{l\,m}$ are determined by requiring that ψ_k^s and its derivative at R from Eq. (4) be continuous to those obtained from Eqs. (6) and (7). One finds

$$C_{l\,m} = e^{i[\delta_l^s(E) - \delta_l(E)]} \frac{N_l^s(K, R)}{N_l(K, R)} a_{l\,m}(k), \tag{8}$$

$$b_{l\,m} = i^{l+1} e^{i\delta_l(E)} \sin[\delta_l^s(E) - \delta_l(E)] \frac{1}{N_l(K, R)} a_{l\,m}(k).$$

The total displaced electron density $\delta\rho_s(\vec{r})$ may be easily obtained through the relation

$$\delta\rho_s(\mathbf{r}) = \frac{2\Omega_0}{8\pi^3} \int dE \int \frac{dS_k}{|\nabla_k E_k|} \delta\rho_k(\vec{r}), \tag{9}$$

where the inside integral is over the constant energy surface defined by the relation $E = E_k$, $\delta\rho_k = |\psi_k^s|^2 - |\psi_k|^2$, Ω_0 is the volume of the unit cell, and the factor of 2 arises due to the spin degeneracy.

Neglecting the anisotropy in $\delta\rho_s(\vec{r})$, Eq. (9) can be rewritten as

$$\delta\rho_s(r) = \sum_l \int \delta\rho_l(r, E) dE, \tag{10}$$

where $\delta\rho_l(r, E)$ can now be related to the partial densities of states (PDOS), $D_l(E)$, of different angular momentum types at the solvent atom site

$$\delta\rho_l(r, E) = D_l(E) S_l(E, r)/Q_l(E), \tag{11}$$

where

$$D_l(E) = \frac{2\Omega_0}{(2\pi)^3} \int \frac{dS_k}{|\nabla_k E_k|} \frac{1}{4\pi} \sum_m |a_{l\,m}(k)|^2 Q_l(E), \tag{12}$$

$$Q_l(E) = \int_0^R R_l^2(E, r) r^2 dr, \tag{13}$$

and

$$S_l(E, r) = \left| \frac{N_l^s(K, R)}{N_l(K, R)} R_l^s(E, r) \right|^2 - |R_l(E, r)|^2, \quad r < R$$

$$= \frac{\sin[\delta_l^s(E) - \delta_l(E)]}{|N_l(K, R)|^2} \times \{ \sin[\delta_l^s(E) + \delta_l(E)][n_l^2(Kr) - j_l^2(Kr)] - 2\cos[\delta_l^s(E) + \delta_l(E)] j_l(Kr) \}, \quad r > R. \tag{14}$$

We thus note that $\delta\rho_s(r)$ is dependent directly on the PDOS at the solvent atom site and the phase shifts δ_l and δ_l^s. In calculating $\delta\rho(r)$ for $r > R$ we have, however, neglected the backscattering from the neighboring atomic sites which is generally a second-order correction.

So far only the contribution from the conduction-band states to the displaced electron density has been considered. If virtual bound states are formed in the conduction band with some solutes their contribution is included in $\delta\rho_s(r)$. However, if the potential of the solute is attractive enough and bound states are formed below the bottom of the conduction band their contribution is not included.[34] For these states the energy E (measured from the zero outside the muffin-tin sphere) is negative and the phase shift $\delta_l^s(E)$ satisfies the condition $\tan\delta_l^s(E) = -i$. Defining $K = \sqrt{-E}$, the position of these bound states is obtained from the condition (for $l = 0$),

$$L_0^s(E, R) + 1/R + K = 0, \tag{15}$$

where $L_0^s(E, R) = R_0^s(E, R)/R_0^{s\prime}(E, R)$ is the logarithmic derivative of the solute potential evaluated at energy E. Equation (15) is obtained by requiring that the wave function and its derivative obtained from the solution of the Schrödinger equation inside the muffin-tin sphere match their counterparts from outside at the surface of the sphere. It can be easily verified that the radial wave function outside the muffin-tin sphere is given by

$$R_0(r) = (R/r) e^{-K(r-R)}, \tag{16}$$

which shows that for $r > R$ the bound state wave function decays exponentially. Note that $R_0(r)$, along with the solution from inside the sphere, has to be normalized so that there are two electrons in the bound state. Their contribution to $\delta\rho(r)$, the total displaced electron density, will be denoted by $\delta\rho_b(r)$.

The third contribution to $\delta\rho(r)$ arises from the difference in the structure of the core electrons of the solute and solvent atoms. However, due to the tightly bound nature of these electrons we have found this to be negligible, and as such it will not be discussed further.

The potential $\delta v(r)$ due to the excess charge den-

sity $\delta\rho(r)$ and the compensating positive charge δZ can now be calculated from the solution of the Poisson equation and is given by (in Rydberg atomic units)

$$\delta v(r) = 8\pi \int_r^\infty (1 - r'/r) r' \delta\rho(r') dr' , \qquad (17)$$

where we have used the charge neutrality condition

$$\delta Z = \int_0^\infty 4\pi r^2 \delta\rho(r) dr . \qquad (18)$$

III. ELECTRONIC STRUCTURE OF THE SOLUTES IN Ni

As we have shown, the electron-density perturbation introduced by the solute plays the central role in our model and governs its interaction with other defects in the lattice. This perturbation is in turn dependent on the partial DOS of the host matrix and the phase shifts of the solute and the host-atom potentials. For this purpose the band structure of the host metal has been calculated using the APW method.[27-29] A lattice constant of $a = 6.6595$ a.u. for Ni at room temperature and a muffin-tin radius of $R = 2.3265$ a.u., which is very close to one-half the nearest-neighbor separation, have been used. The crystal potential was constructed in a standard manner[29] from a superposition of Herman-Skillman[35] self-consistent Hartree-Fock-Slater atomic charge densities obtained with the atomic configuration $3d^9 4s^1$ and atomic potentials that were derived from the solution of the Poisson equation. In the construction of both atomic and crystal potentials the Slater $X\alpha$ exchange approximation was employed, the value of α taken being $\alpha = 1.0$. This choice of the value of α was dictated by the fact that the results from a self-consistent band-structure calculation with $\alpha = \frac{2}{3}$, which is presumably the better value for a metallic solid, are very close to those from a non-self-consistent calculation with $\alpha = 1.0$.[36] The potential inside each muffin-tin sphere was made spherically symmetric. Recent calculations have shown this to be a reasonable approximation. In the interstitial region the potential was not assumed constant in the calculation of the energy bands and wave functions, even though the variation is small. However, all energies are measured from the average potential in the interstitial region as the reference energy. This means that the crystal potential inside and outside the muffin-tin spheres was shifted by a constant V_0 ($V_0 = -1.368$ Ry for Ni) so that the average potential is zero within the interstitial region. Details of the APW method have been discussed by several authors.[28,29]

In Fig. 1 the energy bands of Ni have been plotted in several symmetry directions. The bottom of the conduction band (at Γ_1) is found to be at 0.007 Ry, and the Fermi level falls at $E_F = 0.595$ Ry. The important feature to note in Fig. 1 is an s-type band starting from Γ_1 which strongly hybridizes with the d bands which span in the energy range approximately from 0.32 to 0.62 Ry and have a width of $\simeq 0.30$ Ry. The Fermi level falls in the top portion of the d-band complex. The total DOS, shown in Fig. 2, displays several peaks which are characteristic of the d-band densities of states and can be identified with the critical points in the band structure. The partial DOS analysis, also shown in Fig. 2, within the muffin-tin sphere of Ni shows that the high DOS in the middle of the band structure are due to the d bands. By contrast the s- and p-type DOS are rather small. It can be seen that the s DOS is important only at the bottom portion of the band structure, but at the Fermi energy practically all of the DOS is d-like. In this respect the case of Cu is substantially different from that of Ni. In Cu, with one more electron than in Ni, the d bands are completely filled and the DOS at the Fermi energy is largely s-like. This feature can be seen from the band structure of Ni, where we see that there is a sharp drop in the DOS above the Fermi energy. Let us note, however, that even in Cu the s band hybridizes strongly with the d band, and this has important implications for the interaction energy of a solute with other defects in Cu.

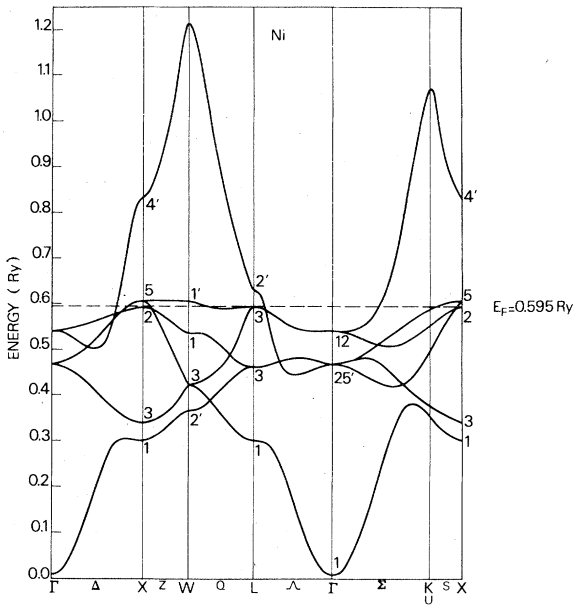

FIG. 1. Energy bands of paramagnetic Ni along several symmetry directions.

In order to investigate the changes in the elec-

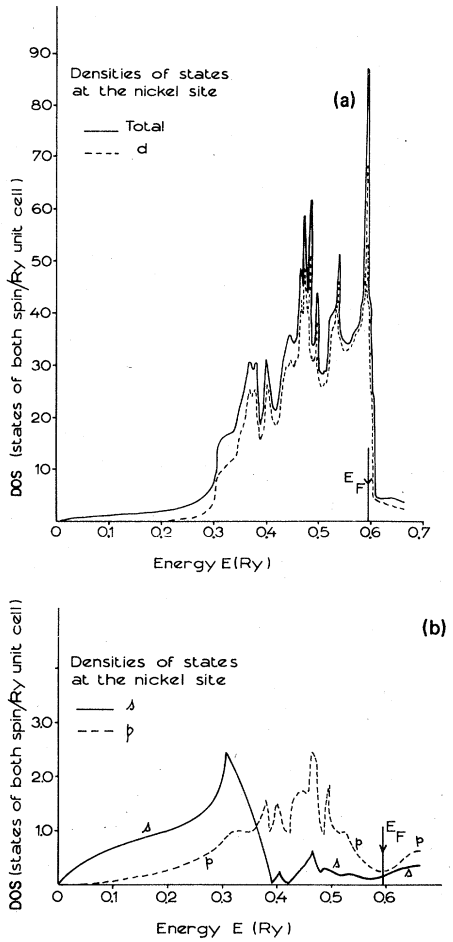

FIG. 2. (a) Total DOS of both spin in states/Ry unit cell; partial DOS of d type in the Ni muffin-tin sphere is shown by dashed curve. (b) Partial s and p DOS in the muffin-tin sphere. Note the dominant nature of the d DOS.

tronic structure which are induced by the solute, the potential of the solute was constructed in the following manner. The atomic charge density of the solute was calculated self-consistently in the Hartree-Fock-Slater approximation from the Herman-Skillman[35] program with the Slater exchange parameter $\alpha=1.0$. From this charge density an atomic potential of the solute was derived by solving the Poisson equation. The potentials of the neighboring 14 shells of Ni atoms were superposed on to the potential of the solute. The corrections for exchange and correlation were again included in the Slater approximation with $\alpha=1.0$. This potential was shifted by the constant V_0, where V_0 is the average potential in the interstitial region for the Ni matrix, so that the potential could be assumed zero in the interstitial region.

In Fig. 3 we have shown the partial DOS at the Si site calculated using the formalism developed in

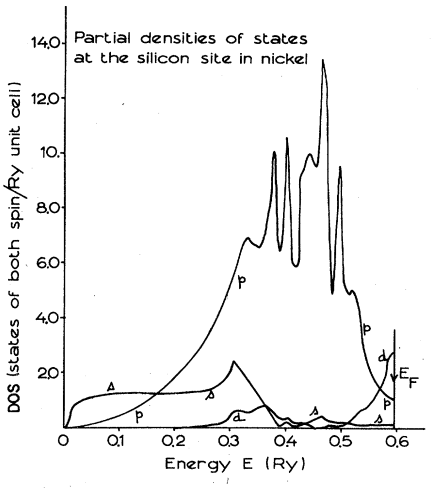

FIG. 3. Partial s, p, and d DOS of both spin in states/Ry unit cell at the Si site in Si muffin-tin sphere. Note that the d DOS at the Si site is small.

Sec. II. Here again, as in Fig. 2, the contribution from the electrons inside the muffin-tin sphere is shown. Let us recall here that in our model the radius of the muffin-tin sphere at the solute atom site is the same as that at the solvent atom site. We find a rather drastic drop in the d DOS at the Si site. This is accompanied by a large increase in the p DOS. This is consistent with the fact that in the outer shell of a Si atom (configuration $3s^2 3p^2$) there are only s and p electrons and no d electrons. Not much change is found in the s DOS in the conduction band. However, a bound state at $E=-0.057$ Ry (i.e., 0.064 Ry below the bottom of the Ni conduction band) is also obtained. This state is of s type and contains two electrons due to the spin degeneracy.

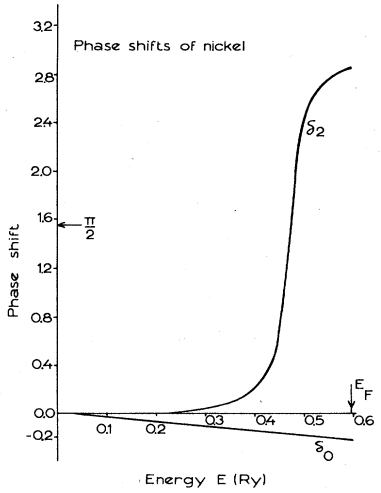

FIG. 4. s- and d-wave phase shifts of Ni as a function of energy.

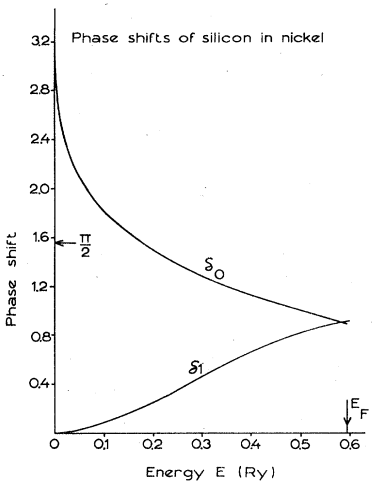

FIG. 5. s and p phase shifts of the potential at the Si site.

Some of the features of the electronic structure may also be inferred from the phase shifts of the potential. In Figs. 4 and 5 we have plotted the phase shifts of the Ni and Si potentials as a function of energy. In the case of Ni the p-wave phase shift has not been shown (Fig. 4) since it is practically negligible at all energies. The s-wave phase shift also turns out to be rather small. The dominant character of the d-wave phase shift can be clearly seen in Fig. 4. At the bottom of the band, up to $\simeq 0.30$ Ry, δ_2 is almost negligible, which is consistent with the fact that there are no d bands in this energy range. As we pointed out before, the d bands start from $\simeq 0.32$ Ry, and one can see that there is an abrupt increase in δ_2 at this energy. It passes quickly through resonance ($\delta_2 = \pi/2$) at $E = 0.473$ Ry indicating the middle of the d-band complex. That the middle of the d-band complex occurs at $E \simeq 0.47$ Ry is quite obvious from Fig. 1. It then attains a value of $\delta_2 = 2.87$ at the Fermi energy which indicates that the d bands are nearly filled in Ni and that the Fermi energy falls at the top of the d bands. In the case of Si the situation is reversed. The d-wave phase shift is always small and hence has not been plotted in Fig. 5. The s-wave phase shift has a value close to π at the bottom of the band which indicates that the potential at the Si site is attractive enough that two s electrons form a bound state below the bottom of the conduction band. The p phase shift is quite large, especially at the Fermi energy, which points toward a significant p-electron density in the conduction band at the Si site. In Table I we have listed the values of the phase shifts of Ni and the solutes Si, Ge, and Be in Ni at the Fermi energy of Ni. The rather large variation of the phase shifts below the

TABLE I. s, p, d phase shifts of Ni, Si, Ge, and Be in Ni matrix evaluated at the Fermi energy of Ni.

	s	p	d
Ni	−0.2226	0.0295	2.8658
Si	0.8978	0.9195	0.0634
Ge	0.9441	0.8467	0.0299
Be	0.2187	0.4769	0.0128

Fermi energy obtained in our calculation indicates that the approximation of slowly varying phase shifts implicit in previous calculations[24] may not be adequate.

The important role played by the electronic structure of the solute in a matrix, i.e., the partial DOS and the phase shifts throughout the Fermi sea, in determining the nature of its interactions with other defects in the solid has already been outlined in detail in Sec. II. To assure maximum accuracy a mesh of $\Delta E = 0.002$ Ry was used in all our calculations and the partial DOS shown in Figs. 2 and 3 were calculated by performing numerical integrations over the corresponding constant energy surfaces. As discussed previously, from the partial DOS the $\delta\rho_s(r)$, the electron density displaced by the solute, may be calculated. This is shown in Fig. 6 for Si in Ni. Let us note that $\delta\rho_s(r)$ represents the contribution of only the states in the conduction band to the perturbation created by the solute. In Fig. 7 is shown the associated electronic potential $\delta V_s(r)$ calculated from $\delta\rho_s(r)$. $\delta V_s(r)$ includes the contribution of the compensating nuclear charge at the solute site. Both $\delta\rho_s(r)$ and $\delta V_s(r)$ display the characteristic Friedel oscillations and are found to be long range. Although $\delta\rho_s(r)$ is relatively small for $r \gtrsim 30$ a.u., a small amount of charge still remains beyond this distance. Its contribution to $\delta V_s(r)$ has been obtained by taking the asymptotic limit of the Bessel and Neumann func-

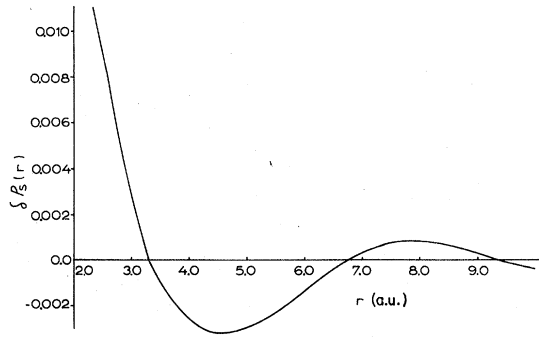

FIG. 6. Electron density $\delta\rho_s(r)$ displaced by Si in Ni (in atomic units) from the conduction-band states.

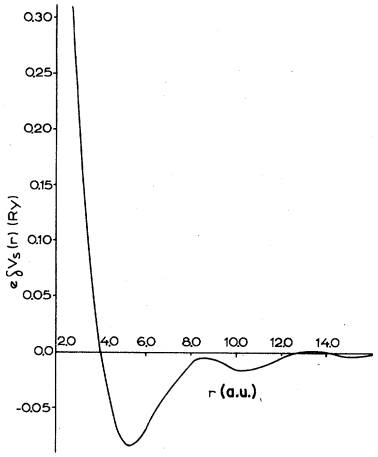

FIG. 7. Potential, $e\delta V_s(r)$ (in Ry), experienced by an electron due to the charge distribution $\delta\rho_s(r)$ and the compensating positive charge of Si in Ni.

tions in Eq. (23), performing the integration over r for $r > 30$ a.u. analytically, and then integrating over E in Eq. (18) numerically. It was found that the total charge associated with $\delta\rho_s(r)$ does not exactly cancel the excess charge at the nucleus, and a small difference remains. $\delta\rho_s(r)$ was therefore renormalized so that this discrepancy is removed. If we compare Figs. 6 and 7 we notice that although $\delta V_s(r)$ has an oscillatory behavior as does $\delta\rho_s(r)$, the nodes in $\delta V_s(r)$ do not appear at the same positions as do those in $\delta\rho_s(r)$, and the form of $\delta V_s(r)$ is substantially different from that of $\delta\rho_s(r)$. This is in contrast to the model of Blandin and Déplanté[24] where the nodes in $\delta V_s(r)$ and $\delta\rho_s(r)$ appear at exactly the same positions and their forms are identical except for a multiplicative factor.

In Fig. 8 are shown the charge density $\delta\rho_b(r)$ and the potential $\delta V_b(r)$ associated with the s bound state at the Si site. Again, $\delta V_b(r)$ includes the contribution of the compensating nuclear charge at the Si site. We note that $\delta\rho_b(r)$ and $\delta V_b(r)$ both have exponentially decaying behavior which is characteristic of bound states. This is in contrast to $\delta\rho_s(r)$ and $\delta V_s(r)$ which are oscillating. This will be seen to be important in determining the interaction of Si with vacancies and interstitials in Ni.

The electronic structure of Ge in Ni is very similar to that of Si in Ni. For this reason the detailed results will not be presented for Ge. There are important differences, however, which result in their changed interactions with vacancies and interstitials. First, the bound state in Ge is somewhat more tightly bound than in Si. We find it to be situated at $E = -0.090$ Ry (i.e., 0.097 Ry below the bottom of the Ni conduction band). This

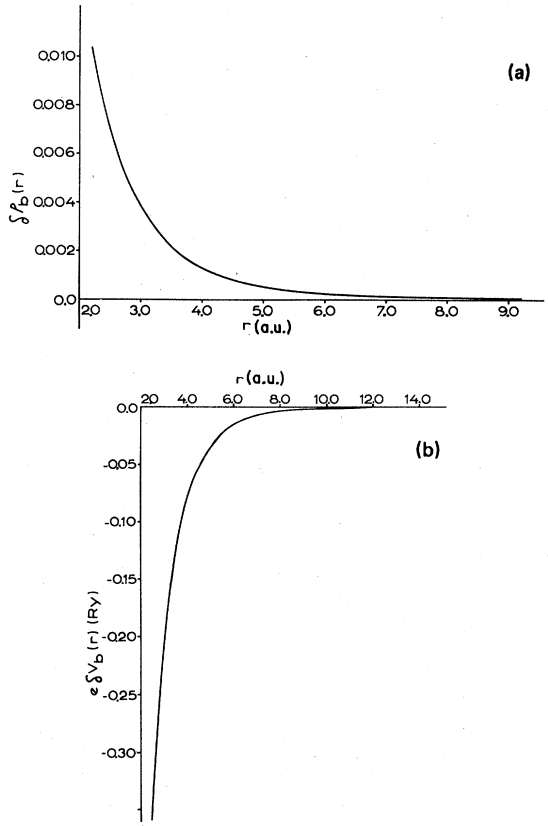

FIG. 8. (a) Charge distribution $\delta\rho_b(r)$ associated with the bound s state in Si in Ni. (b) Potential, $e\delta V_b(r)$, due to the bound-state electrons in Si plus the compensating positive charge.

is $\simeq 0.45$ eV lower than found for Si. This difference may be attributed partly to the fact that even in the atomic state the 4s electrons in Ge are somewhat more tightly bound than the 3s electrons of Si. Second, although $\delta V_s(r)$ in Ge looks quite similar to its counterpart in Si, for example, the nodes in $\delta V_s(r)$ in the case of Ni(Ge) are obtained at essentially the same positions as in Ni(Si), there are nonetheless differences in the magnitudes of $\delta V_s(r)$ in the two cases. Even though these differences are not large in absolute magnitude they are relatively large in the region which governs the interaction of the solute with other defects. Furthermore, they cannot be simulated by either a shift in $\delta V_s(r)$ or by a constant multiplication factor. They are found to be rather strongly spatially dependent. The fact that the bound state in Ge lies lower than in Si results in a bound-state potential $\delta V_b(r)$ that is less extended and less attractive for an electron in the case of Ge than in Si. This difference, coupled with the differences in $\delta V_s(r)$, is indeed large enough to alter the nature of the two solutes *vis a vis* vacan-

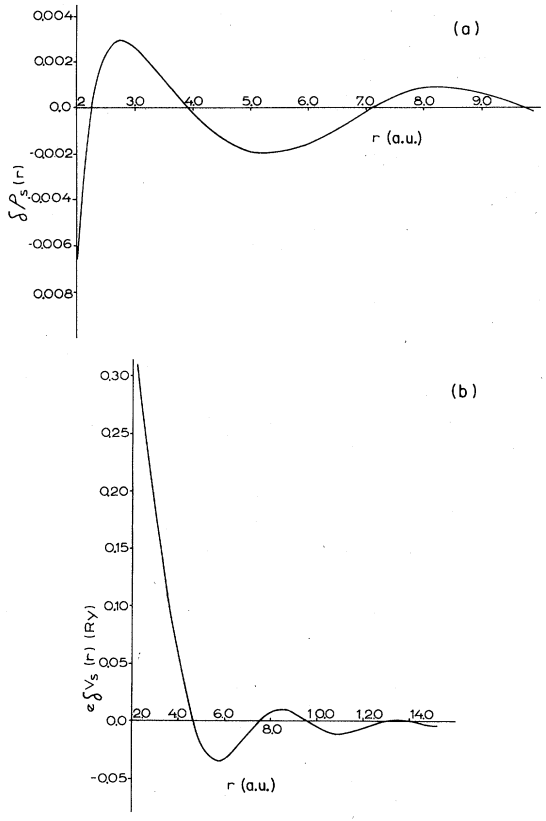

FIG. 9. (a) Electron density $\delta\rho_s(r)$ displaced by Be in Ni from the conduction-band states. (b) Potential, $e\delta V_s(r)$, experienced by an electron due to the charge distribution $\delta\rho_s(r)$ and the compensating positive charge of Be in Ni.

cies and interstitials, especially the latter. This point will be further discussed in Sec. IV.

In the case of *Ni*(Be) no bound state is formed. $\delta\rho_s(r)$ and $\delta V(s)$ are shown in Fig. 9 for this case. We can see clearly that $\delta\rho_s(r)$ and $\delta V_s(s)$ are both substantially different from their counterparts for Si and Ge. This is something which is not unexpected, noting the differences in their electronic configurations. Let us note also that the nodes in $\delta\rho_s(r)$ and $\delta V_s(r)$ are found in significantly different positions than for Si and Ge.

IV. SOLUTE-VACANCY AND SOLUTE-INTERSTITIAL BINDING ENERGIES

In Table II are given the solute-vacancy binding energies for Si, Ge, and Be solutes in Ni calculated up to the fifth-neighbor distance of a vacancy from the solute. The vacancy in this calculation is represented by the absence of an atom. The charge distribution inside the Wigner-Seitz sphere of the vacancy is obtained from band-structure calculation and assumed to be spherically symmetric.[37] Two observations may be made for the case of Si and Ge. First, even though the nearest-neighbor configuration is found to be the most stable one, the interaction between the solute and a vacancy extends to large distances and remains non-negligible even at the fifth-neighbor separation. In particular the binding energy at the second-neighbor position is comparable to that at the nearest-neighbor one. Second, the interaction at the nearest-neighbor site is rather strong with binding energies of 0.73 and 0.55 eV, for Si and Ge, respectively. In an effort to understand the origin of this behavior, separate contributions from the bound s states below the conduction band and the scattering states in the conduction band have also been listed in Table II. Contribution from the core states is not shown since it is found to be negligible even at the nearest-neighbor separation, owing to the tightly bound nature of the core electrons. Each separate contribution includes the terms associated with the corresponding electron-density perturbation and the compensating nuclear charge at the solute site. We see that the strong interaction at the nearest-neighbor site for Si and Ge is due entirely to the

TABLE II. Solute-vacancy binding energy E^b_{vs} (in eV) in Ni for Si, Ge, and Be solutes calculated up to the fifth-neighbor separation. The positive sign indicates attraction or binding. In the case of Si and Ge the labels b and s refer to the contributions from the bound- and the conduction-electron scattering states, respectively, and t is the total binding energy. For Be there are no bound states and all the binding is due to conduction-electron states.

Solute		First neighbor	Second neighbor	Third neighbor	Fourth neighbor	Fifth neighbor
Si	b	0.743	0.157	0.053	0.022	0.011
	s	−0.013	0.454	0.298	0.156	0.094
	t	0.730	0.611	0.351	0.178	0.105
Ge	b	0.508	0.083	0.023	0.008	0.003
	s	0.041	0.410	0.250	0.122	0.070
	t	0.549	0.493	0.273	0.130	0.073
Be	t	−0.323	0.055	0.072	0.031	0.018

bound states. At higher separations the bound-states contribution has dropped off sharply, reflecting their exponentially decaying behavior, and most of the contribution to the interaction energy comes from the scattering states. This is the interplay of the bound- and scattering-states contributions, which are inherently of different nature, thus making the binding energies at the nearest- and the next-nearest-neighbor positions comparable. For the case of Be we find a repulsive interaction between the solute and a vacancy in the nearest-neighbor configuration. At second- and higher-neighbor separations a small binding is obtained.

In Table III the binding energies of the solute-interstitial pair in the ⟨100⟩ mixed-dumbbell configuration are presented. Separate contributions from the core, bound, and the scattering states have also been listed in Table III. In this calculation we assume when an atom of the matrix goes into the interstitial position it rigidly carries its screening charge with it. The interstitial atom is represented by a neutral Wigner-Seitz sphere and the conduction-electron density inside it obtained from the band-structure calculation. A separation of 0.55 a (where a is the lattice constant) between the two atoms of a ⟨100⟩ mixed dumbbell is used from the diffuse x-ray scattering measurements of Haubold and Martinsen[38] on Cu. Again the contribution from the core states is rather small for all three solutes Si, Ge, and Be. As in the case of Be where there is no bound state, practically all of the contribution to the binding energy comes from the scattering states in the conduction band, and a binding energy of 0.583 eV is obtained. In the case of Si and Ge the bound- and scattering-state contributions are large and of opposite sign. The net result is a binding energy of 0.898 eV in the case of Si and a small binding energy of 0.276 eV for Ge. Thus our calculations indicate the formation of ⟨100⟩ mixed dumbbells for all the three solutes studied here. To facilitate comparison with the model of Dederichs[2] the linear size factors of these solutes in Ni have been listed in Table III. The Dederichs model would predict positive binding energies for Si and Be solutes, while for Ge the binding energy would be negative and the mixed dumbbell would not be formed. Furthermore, in his model the binding energies are essentially proportional to the linear size factor. Table III shows that this rule does not hold.

Since no direct experimental measurements of either the solute-vacancy or the mixed-dumbbell binding energies in Ni for the solutes studied here exist, to our knowledge, in the literature, direct comparison with experiment is not possible at this stage. Even though our calculated values of the solute-vacancy binding energies of 0.73 eV in Ni(Si) and 0.55 eV in Ni(Ge) may seem high it should be noted that the formation energy E_{fv}^{f} of a vacancy in Ni, $E_{fv}^{f} = 1.60 \pm 0.05$ eV,[39] with which the comparison is more appropriate, is also rather high. By comparison, the value of E_{fv}^{f} for Al is only 0.66 ± 0.03 eV.[40] The example of Al is taken here since this is a metal where the solute-vacancy interactions have been most studied. On the basis of these studies a conclusion has been drawn that the solute-vacancy binding energies are quite small. We note here that even in Al the interaction with transition-metal solutes, where one expects the interaction to be particularly strong, has not received much attention. There is no *a priori* reason for the vacancy-solute interaction to be weak, and the experimental evidence for a rather strong interaction has recently been provided by Berger and Siegel[41] in Cu(Sc). These authors studied the effects of the addition of trace amounts (12–96 at ppm) of Sc upon the annealing kinetics of high-purity Cu quenched from 600–700 °C. They concluded the interaction enthalpy of the solute-vacancy complex is of the order of the vacancy formation enthalpy in Cu, 1.30 eV.

Recently, Doyama *et al.*[42] have studied the interaction of Ge solutes with vacancies in Cu by positron annihilation and have deduced a value of 0.27 ± 0.10 eV for the binding energy. This will be consistent with our results on Ni(Ge). As we have noted, the vacancy-solute binding in Ni(Ge) in the nearest-neighbor configuration in our calculation, 0.55 eV, is derived entirely from the bound-state contribution. Now the bound state in

TABLE III. Solute-interstitial binding energy E_{IS}^{b} (in eV) in Ni for Si, Ge, and Be solutes in the ⟨100⟩ mixed dumbbell configuration. The positive sign indicates binding.

Solute	Contribution from Core states	Bound states	Conduction-electron states	Total	Linear size factor of the solute
Si	−0.031	2.669	−1.740	0.898	−0.0198
Ge	0.054	2.636	−2.414	0.276	0.0468
Be	−0.035	0.0	0.618	0.583	−0.130

Cu(Si) lies lower in energy[43] than in *Ni*(Si) by ≃1 eV relative to the bottom of the host-metal conduction band. This is presumably due to the fact that Cu, with one more electron than Ni, contributes a more attractive potential at the Si site. This lowering of the bound-state energy level will result in a quite substantially reduced contribution to the interaction energy. The contribution from the scattering states is more difficult to estimate. However, if we assume that it is not much affected at the nearest-neighbor vacancy site, we can assume then that the Si-vacancy binding energy in Cu will be significantly smaller than in *Ni*(Si). In our calculation we have found that the bound state lies lower in *Ni*(Ge) than in *Ni*(Si). It will also be true for *Cu*(Ge) and *Cu*(Si) for the same reasons, namely, that the 4*s* electrons in Ge, even in the atomic state, lie somewhat lower than the 3*s* electrons in Si. Thus we expect the Ge-vacancy binding energy to be lower than the Si-vacancy binding energy in Cu. As a result the experimental value obtained by Doyama *et al.* for *Cu*(Ge), which shows that the binding energy of vacancy with Ge is lower than the value obtained in our calculation for *Ni*(Ge), is consistent with our model.

A similar comparison with our calculated mixed-dumbbell binding energies is not possible. Suffice it to say, however, that the radiation-induced solute segregation and precipitation to the sinks in *Ni*(Si) and *Ni*(Be) alloys[44-46] have been interpreted in terms of strong solute-interstitial-atom binding energies. This is consistent with our calculations where we find large mixed-dumbbell binding energies of 0.90 and 0.58 eV for *Ni*(Si) and *Ni*(Be) alloys, respectively. Binding energies of the same order are of course also expected from the simple size-effect considerations. From the size-effect considerations, however, one also expects the mixed-dumbbell binding energy in *Ni*(Ge) to be negative, i.e., the solvent-atom dumbbell would be energetically more stable than the mixed dumbbell. This would indicate solute depletion from the sinks and solute enrichment in the matrix if one assumes a weak vacancy-solute interaction. The experimental evidence, however, points to the contrary. Recent experiments of Barbu[47] show that in undersaturated solid solutions of Ni −6 at.% Ge, precipitation of the solute at the sinks takes place. For this to occur, either of the two following mechanisms will be necessary. If the solute is dragged to the sinks by the flux of the interstitials then it is important that the mixed dumbbell be stable and have a positive binding energy.[19,48] On the other hand if the solute segregation to the sinks occurs via the vacancy wind mechanism suggested by Anthony,[49] then it is necessary that the solute-vacancy binding energy be not only positive but large. Our calculations indicate that in *Ni*(Ge) quite likely both mechanisms operate simultaneously, since we find a significant Ge-vacancy binding energy, $E_{VS}^{b} = 0.55$ eV, and a positive, although small, mixed-dumbbell binding energy $E_{IS}^{b} = 0.28$ eV. However, because of the much larger vacancy-solute binding as compared to the interstitial-solute binding, the vacancy wind mechanism will be expected to dominate.

Barbu[47] has also observed the formation of voids in *Ni*(Ge) under irradiation. This is in contrast to the case of *Ni*(Si) where voids do not form. This difference in their behavior may, in part, be related to the fact that in *Ni*(Si) the binding energy of the solute with both vacancies and interstitials is large. This probably leads to enhanced recombination of vacancies and interstitials in the neighborhood of the solute. The same will not be expected in *Ni*(Ge) where the solute-interstitial binding energy is relatively small.

V. CONCLUSION

In this paper an attempt was made to assess the role of the electronic structure of the solute in dictating its interactions with other point defects in the lattice. Previous calculations of the solute-interstitial binding energies have been based on the empirical correlations with the size of the solute in a matrix. We have shown that this criterion is too simple and the size of the solute alone is not enough to determine the nature of its interactions with an interstitial atom. Si and Be, both undersized in Ni, are found to have large positive binding energies in the mixed-dumbbell configuration. This is also expected from the size-effect consideration. However, Ge, which is oversized in Ni, is also found to have a positive binding energy, although small, in the mixed-dumbbell configuration. This is not expected from the size-effect considerations. Both Si and Ge have been also found to have significant binding energies with vacancies. Recent experimental work by Barbu[47] on *Ni*(Ge) seem to point toward the general validity of our results. In our calculations the relaxation of the lattice due to the size of the solute are not included. These will obviously modify somewhat the results obtained in the present work. However, we do not expect them to be large enough to change either the nature of our results or the conclusions drawn from them. With the binding energies presented in this paper the radiation-induced segregation and precipitation has recently been calculated[50] using the Johnson-Lam model.[19] The results are in excel-

lent agreement with the experimental data on precipitation in both *Ni*(Si) and *Ni*(Ge) alloys.

ACKNOWLEDGMENTS

The author is indebted to Dr. Y. Adda for suggesting this problem and for his constant interest and support. The author is also pleased to acknowledge frequent and fruitful discussions with Dr. Y. Adda, Dr. G. Martin, Dr. A. Barbu, Dr. N. Q. Lam, and Dr. G. Brébec.

[1]H. Wollenberger, J. Nucl. Mater. 69-70, 362 (1978).
[2]P. H. Dederichs, C. Lehmann, H. R. Schober, A. Scholz, and R. Zeller, J. Nucl. Mater. 69-70, 176 (1978).
[3]J. Hillairet, in *Défauts Ponctuels dans les Solides* (Les Editions de Physique, Orsay, France, 1977), p. 417.
[4]R. Paulin, Ref. 3, p. 257.
[5]R. W. Balluffi and P. S. Ho, *Diffusion* (American Society for Metals, Metals Park, Ohio, 1973), p. 83.
[6]N. H. March and J. S. Rousseau, Cryst. Lattice Defects 2, 1 (1971).
[7]M. Doyama, J. Nucl. Mater. 69-70, 350 (1978).
[8]L. E. Rehn, K. H. Robrock, and H. Jacques, J. Phys. F 8, 1835 (1978).
[9]J. Burke, J. Less Common Met. 28, 441 (1972).
[10]N. H. March, J. Nucl. Mater. 69-70, 490 (1978).
[11]P. R. Okamoto and H. Wiedersich, J. Nucl. Mater. 53, 336 (1974).
[12]N. Q. Lam, P. R. Okamoto, and H. Wiedersich, J. Nucl. Mater. 74, 101 (1978).
[13]H. W. King, J. Mater. Sci. 1, 79 (1966).
[14]R. A. Johnson (private communication to N. H. March, Ref. 6, p. 499).
[15]R. A. Johnson, G. J. Dienes, and A. C. Damask, Acta Metall. 12, 1215 (1964).
[16]M. L. Swanson, L. M. Howe, and A. F. Quenneville, J. Nucl. Mater. 69-70, 372 (1978).
[17]G. G. Setser, K. L. Hultman, J. Holder, and A. V. Granato, Bull. Am. Phys. Soc. 24, 242 (1979).
[18]A. D. Marwick, R. C. Piller, and P. M. Sivell, J. Nucl. Mater. 83, 35 (1979).
[19]R. A. Johnson and N. Q. Lam, Phys. Rev. B 13, 4364 (1976).
[20]P. S. Ho and R. Benedek, J. Nucl. Mater. 69-70, 730 (1978).
[21]R. P. Gupta, Philos. Mag. B 41, 169 (1980).
[22]R. Yamamoto, O. Takai, and M. Doyama, J. Nucl. Mater. 69-70, 727 (1978).
[23]A. Blandin, J. L. Déplanté, and J. Friedel, J. Phys. Soc. Jpn. 18, Suppl. II, 85 (1963).
[24]A. Blandin and J. L. Déplanté, J. Phys. Chem. Solids 26, 381 (1965).
[25]L. C. R. Alfred and D. O. Van Ostenburg, Phys. Lett. 26A, 27 (1968).
[26]A. D. Le Claire, J. Nucl. Mater. 69-70, 70 (1978).
[27]J. M. Ziman, Solid State Phys. 26, 1 (1971).
[28]J. O. Dimmock, Solid State Phys. 26, 103 (1971).
[29]T. L. Loucks, *Augmented Plane Wave Method* (Benjamin, New York, 1967).
[30]G. J. Morgan, Proc. Phys. Soc. London 89, 365 (1966).
[31]P. T. Coleridge, N. A. W. Holzwarth, and M. J. G. Lee, Phys. Rev. B 10, 1213 (1974).
[32]R. P. Gupta and R. Benedek, Phys. Rev. B 19, 583 (1979).
[33]W. Kohn and S. H. Vosko, Phys. Rev. 119, 912 (1960).
[34]R. H. Lasseter and P. Soven, Phys. Rev. B 8, 2476 (1973).
[35]F. Herman and S. Skillman, *Atomic Structure Calculations* (Prentice-Hall, Englewood Cliffs, New Jersey, 1963).
[36]S. H. Liu, in *Handbook on the Physics and Chemistry of Rare Earths*, edited by K. A. Gschneidner and L. Eyring (North-Holland, New York, 1978).
[37]R. P. Gupta and R. W. Siegel, Phys. Rev. Lett. 39, 1212 (1977).
[38]H. G. Haubold and D. Martinsen, J. Nucl. Mater. 69-70, 644 (1978).
[39]G. Dlubek, O. Brummer, and N. Meyendorf, Phys. Status Solidi 39, K 95 (1977).
[40]M. J. Fluss, L. C. Smedskjaer, M. K. Chason, D. G. Legnini, and R. W. Siegel, Phys. Rev. B 17, 3444 (1978).
[41]A. S. Berger and R. W. Siegel, J. Phys. F 9, L67 (1979).
[42]M. Doyama, K. Kuribayashi, S. Nanao, and S. Tanigawa, Appl. Phys. 4, 153 (1974).
[43]K. Terakura, J. Phys. Soc. Jpn. 40, 450 (1976).
[44]A. Barbu and A. J. Ardell, Scr. Metall. 9, 1233 (1975).
[45]A. Barbu and G. Martin, Scr. Metall. 11, 771 (1977).
[46]P. R. Okamoto, A. Taylor, and H. Wiedersich, Proceedings of the International Conference on Fundamental Aspects of Radiation Damage in Metals, Gatlinburg, Tenn., Vol. II, 1188 (1975).
[47]A. Barbu, International Conference on Irradiation Behavior of Metallic Materials for Fast Reactor Core Components, Ajaccio, France, June 1979, p. 69.
[48]A. Barbu, Acta Metall. 28, 499 (1980).
[49]T. R. Anthony, Acta Metall. 18, 307 (1970).
[50]R. P. Gupta and N. Q. Lam, Scr. Metall. 13, 1005 (1979).